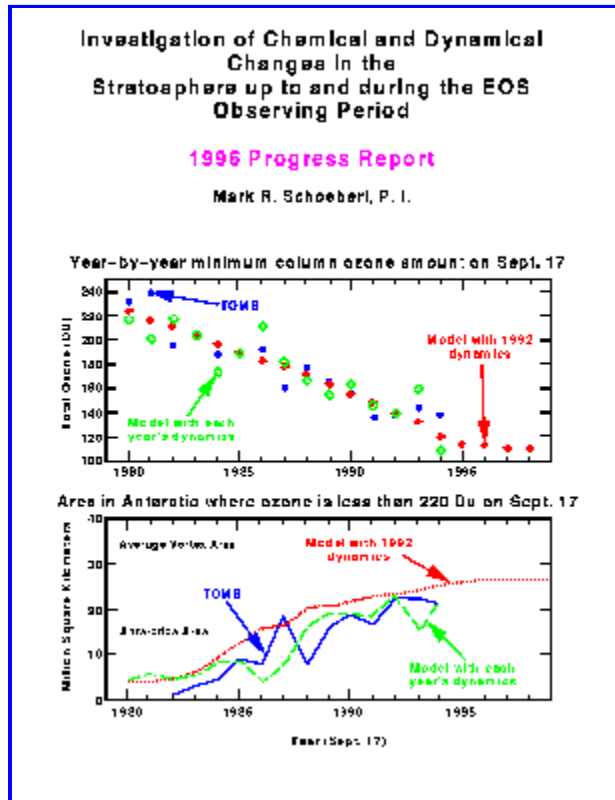


[Return to EOS page](#)

1996 Progress Report on EOS IDS



Investigation of Chemical and Dynamical Changes in the Stratosphere up to and during the EOS Observing Period

M. R. Schoeberl, P. I., *Goddard Space Flight Center*

Steve E. Cohn, *Goddard Space Flight Center*

Anne R. Douglass, *Goddard Space Flight Center*

James Gleason, *Goddard Space Flight Center*

Charles H. Jackman, *Goddard Space Flight Center*

Leslie R. Lait, *Hughes STX, Landover, MD*

Paul A. Newman, *Goddard Space Flight Center*

Richard B. Rood, *Goddard Space Flight Center*

Joan E. Rosenfield, *Goddard Space Flight Center*

Richard S. Stolarski, *Goddard Space Flight Center*

Anne M. Thompson, *Goddard Space Flight Center*

Marvin A. Geller, *State University of New York-Stony Brook*

Robert D. Hudson, *University of Maryland-College Park*

One Page Summary

This report is an update to the more comprehensive [1995 report](#).

Our research efforts achieved the major goal of completing the first of the Multiyear Ozone Depletion Experiments (MODE) which has been recently published in JGR. The goal of MODE is to model the development of the polar ozone depletions using satellite and ground based data. The [cover figure](#) and [Figure 2.2.1-1](#) (and enclosed viewgraph) summarize the Antarctic results of MODE which reproduce the development of the ozone hole. The MODE trajectory technique is now being extended to study the northern hemisphere.

We have also achieved a milestone with our 2D interactive model. Our Pinatubo studies (Figures 2.2.5-1,2) show good agreement with observations - probably the best achieved yet with a 2D model with interactive dynamics. We are now turning our attention to climate studies (CO2 doubling).

The main thrust of the 3D chemical modelling effort (partially supported under this IDS) is to understand the impact of the EOS assimilation winds on the transport of long lived tracers. These studies and direct constituent assimilation studies described below are having a positive impact on the stratospheric assimilation.

Aircraft data analysis has always been a central theme of the proposal. We are now just beginning to analyze the TOTE/VOTE data in conjunction with our ongoing STRAT data analysis. Part of our effort is to focus on tropical dynamics and implications for mixing. We have been modelling the QBO as well as estimation the mixing from the tracer-wind correlations.

Our analysis of tropospheric ozone continues, and we are looking at an improvement to the Fishman residual technique to estimate tropospheric ozone from TOMS and SAGE data. In the first part of this effort, we are building a climatology of lower stratospheric ozone using trajectory mapping (developed under this IDS). We are also approaching the problem using potential vorticity - potential temperature binning. In the text below we describe work with tropical TOMS measurements and estimates of tropospheric ozone from that data.

Using the UARS and aircraft data along with high resolution trajectory studies, we are also investigating the fundamental mixing processes of the stratosphere.

Finally, we continue to support the trajectory automailer which is heavily used by the community (53% increase in 1995 over 1994). The automailer statistics are shown at the end of this report. Eighteen publications were associated with this IDS in FY 1996.

This report is located at http://hyperion.gsfc.nasa.gov/EOS/report_1996/report.html

1.0 Background

Our 1995 report is located on the world-wide web at http://hyperion.gsfc.nasa.gov/EOS/report_1995/report.html

The introduction to the 1995 report summarizes our main research goals and progress up through 1995. This report stands as an update of the 1995 report. The sectional structure is similar to the 1995 report so that the reader can compare this report to the 1995 report section by section except where indicated.

2.0 Scientific Activities

2.1 Multiyear Ozone Depletion Experiment (MODE)

The goal of MODE under this IDS is to simulate the observed long-term change in ozone within the polar vortex. The first phase of this experiment involved simulating the growth of the Antarctic ozone hole. This phase has been completed and published in Schoeberl et al. [1996]. We have now begun to simulate the Arctic ozone loss as described below. The MODE project is central to the IDS goal of isolating anthropogenic and natural changes in ozone.

2.1.1 Antarctic Experiment

To address the Antarctic problem, we concentrated on simulating the UARS observed changes in ozone using the Lagrangian chemistry model. The procedure was as follows: first, Cryogenic Limb Array Talon Spectrometer (CLAES) and Microwave Limb Sounder (MLS) data are mapped into potential vorticity space for data collected on August 17, 1992. Halogen Occultation Experiment (HALOE) HCl data is used from the entire previous month (because HALOE data is collected more slowly than CLAES and MILS data, we have to include the data over a longer period to get sufficient sampling with respect to potential vorticity). The UARS data are then used to initialize the Lagrangian chemical model. The model is then run forward for a month for 625 regularly spaced isentropic trajectories. The isentropic assumption is appropriate for the Antarctic vortex, as diabatic cooling rates are small in late winter. After validating the 1992 ozone loss we ran the model for all the TOMS years to see if we could reproduce the chlorine trends. The year to year variability was difficult to reproduce but the overall development of the ozone hole

The Antarctic MODE results were published in Schoeberl et al. [1996]. [Figure 2.1.1-1](#) shows the long term changes in Antarctic ozone from the MODE Antarctic experiment.

2.1.2 Arctic Experiment

We are now gearing up for a MODE Arctic experiment. To do this, a number of significant model changes had to be made because of the larger diabatic descent. A preliminary January 1993 experiment has been performed. [Figure 2.1.2-1a](#) and [Figure 2.1.2-1b](#) show the results of the experiment, comparing the Arctic ozone loss at a single isentropic level. Future tasks include full diabatic runs and a simplified denitrification scheme.

2.2 Stratospheric Chemical and Dynamical Modeling

This section describes some of the other chemical and dynamical activities supported under this IDS. The testing and development of models as tools for our science objectives and analysis of EOS data is a critical activity in the pre-EOS time frame. Most of our activity centers around analysis of satellite and aircraft data sets.

2.2.1 Simulation of stratospheric constituents using the 3-D chemical model

The three-dimensional chemical model is being developed under funding from the Atmospheric Chemistry Modeling and Analysis Program. The chemical package and transport scheme eventually will be used in the chemical assimilation effort. Thus, scientific testing of the 3-D chemical model is essential for the success of the IDS assimilation program and also allows us to move toward our goal of using the 3-D chemical model for interpreting long-term trends.

There have been substantial improvements to the 3-D chemistry and transport model in the last year. Development of a complete scheme for stratospheric photochemical processes, including gas-phase and heterogeneous reactions and a model for PSC formation, allows a more complete comparison of modeled physical processes with observations. A simulation for the period November 15, 1991-May 31, 1992 has been completed. Ozone, constituents directly important to the ozone evolution such as nitrogen dioxide and chlorine monoxide, and long lived constituents such as nitrous oxide and methane are included in the simulation. Because the winds and temperatures used in this off-line simulation are taken from the GEOS-1 data assimilation system, the calculated constituent evolution is sensibly compared with observations. To date, such comparisons emphasize observations from the UARS satellite.

The performance of this CTM is evaluated by comparison of model and observations through interpolation of model fields to the times and locations of the satellite observations. Scatter plots for 6.8 hPa ozone observations, poleward of 30N and outside the polar vortex, are given for UARS instruments HALOE, CLAES, and MILS in [Figure 2.2.1-1](#). For all three instruments the model values show good correlation with the observations. The model field for February 19 at 7 hPa is given in [Figure 2.2.1-2](#); the model field shows spatial variability outside the tropics and the polar vortex which is reflected in the observations. The model shows two areas of low ozone mixing ratios within the polar vortex and between about 140E and 210E, associated with the Aleutian anticyclone. Manney et al. [1995] examine similar low ozone "pockets" and show that these are most likely produced photochemically. Douglass et al. [1996] confirm that when air is confined to the Aleutian anticyclone the ozone decreases photochemically, and show that horizontal transport is essential to maintain the winter ozone above its photochemical equilibrium mixing ratio at 7 hPa throughout the middle latitudes. This analysis shows that the model ozone evolution at middle latitudes parallels the observed ozone evolution, indicating an appropriate model balance between photochemical processes and horizontal waves transports.

The same analysis reveals flaws in the model transport. The sharp gradients observed by CLAES in long-lived constituents such as nitrous oxide are not maintained by the model, which leads to excessively high model mixing ratios in the subtropics and at middle latitudes. This problem, which is produced by the model wind fields, is being addressed both through improvements in using the assimilation wind fields in the model and through improvements to the assimilation system.

2.2.2 Quasi-biennial Oscillation (new section)

2.2.2.1 Using the QBO to assess mixing

One of the current issues in stratospheric dynamics is the rate at which material mixes into the tropical stratosphere from midlatitudes. It turns out that an upper limit on the rate of mixing can be estimated from the tracer correlations with the tropical QBO winds. [Figure 2.2.2.1-1](#) shows the ratio of N₂O to

CH₄ from CLAES and an overlay of the QBO Singapore. The close correlation of the descent of the QBO zero wind line and the change in the trace gas ratio suggests that little air is mixing in from mid-latitudes. We estimate that the mixing coefficient for air from mid-latitudes is no greater than about $7 \times 10^8 \text{ cm}^2/\text{sec}$ which is much lower than used in most 2D models. These results are in press in GRL [Schoeberl et al., 1996]

We are currently investigating the movement of dry air from the tropics to midlatitudes using high vertical resolution HALOE data from UARS.

2.2.2.2 Models of the QBO

A paper was submitted to and accepted by the Journal of the Atmospheric Sciences titled, "Calculations of the Stratospheric QBO for Time-Varying Wave Forcing", by M. A. Geller, W. Shen, M. Zhang, and W. Wu. The research in this paper started off with the premise that tropospherically forced atmospheric waves in the equatorial region force the observed quasi-biennial oscillation (QBO) in lower stratospheric winds in equatorial regions. This is the accepted mechanism. We then noted that the state of sea-surface temperatures (SSTs), very likely, is important in determining the nature of these equatorial waves. Thus, it is likely that there is a physical link between SSTs and the QBO. Yet, previous studies had indicated that time series of equatorial SSTs appear to be unrelated to QBO behavior. Noting that wave forcing of the QBO is an inherently nonlinear problem, we carried out idealized models (of the nature done earlier by Holton and Lindzen, for example) with sinusoidally varying equatorial wave behavior of different periods. The QBO response differed depending on the ratio of the time varying forcing to the steady forcing, the period of the equatorial wave modulation, and the phase relationship between the time variation of the easterly and westerly momentum fluxes by the waves. We then tried a hypothesized time variation for the equatorial wave momentum fluxes that were straight forwardly related to observed SST variations. Our derived period of the QBO showed little relation to the original time variation of the momentum fluxes (i. e., the SSTs) but did show great resemblance to the observed behavior of the QBO. Thus, we concluded that: (1) In a nonlinear phenomenon, such as the QBO, there is no reason to expect the QBO response to resemble the time variation of the forcing. (2) It is very likely that equatorial SST variations play a large part in controlling the time variation of the QBO. (3) It is likely that the SST control of equatorial wave momentum fluxes results in the easterly and westerly momentum fluxes varying out of phase with one another.

2.2.3 Trajectory Mapping

While SBUV measurements provide daily, near global coverage of ozone, these instruments are unable to provide reliable profiles of ozone below the ozone peak. HALOE and SAGE are high resolution profile instruments and are able to provide information on the shape of the ozone profile below the peak. They both make their measurements, however, using a solar occultation technique. This technique limits measurements to two narrow latitude bands of observations each day: one in the location of sunsets, the other in the location of sunrises. Data coverage, therefore, is relatively sparse.

Combined, the SBUV and HALOE/SAGE data sets provide us with all the information on ozone we desire: global coverage with excellent vertical resolution from the tropopause into the mesosphere. To make the HALOE/SAGE data useful, we need to produce synoptic maps with global coverage. Because ozone behaves like a conserved trace gas in the lower stratosphere, we can apply the trajectory mapping technique [Morris et al., 1995] to an entire month of HALOE or SAGE measurements and produce the desired synoptic maps.

To derive our estimates of column ozone from the HALOE and SAGE measurements, we produce isentropic trajectory maps on eight potential temperature surfaces between 400K (20km) and 1200K

(36km). Most of the ozone can be found between these levels (as shown in [Figure 2.2.3-1](#)). We then advect the measurements from an entire month of sampling to a specified date and time. The data on each level are gridded using a Barnes' scheme and then integrated vertically. [Figure 2.2.3-2](#) shows such a map from a combination of HALOE and SAGE data in September 1994. We have found that combining HALOE and SAGE data for use in the production of a single map is not unwarranted. [Figure 2.2.3-3](#) shows a comparison of HALOE and SAGE measurements from one of the potential temperature surfaces used for the integration. The agreement between HALOE and SAGE is quite good with only a small offset. Similar agreement is observed at other vertical levels. [Figure 2.2.3-4](#) shows the TOMS total ozone field for the same date as the combine HALOE/SAGE field shown in [Figure 2.2.3-2](#). Good agreement between the features in the two data sets is apparent. The lack of inclusion of tropospheric ozone in the HALOE/SAGE map is largely responsible for the observed offset although systematic bias between HALOE/SAGE and TOMS must also be considered.

Our future research on this project will be directed toward a number of goals: to expand our technique and produce combined HALOE/SAGE/SBUV2 profiles; to improve the first guess profiles for the SBUV2 retrievals; to derive tropospheric ozone through a subtraction of our stratospheric column maps of HALOE/SAGE from the TOMS total ozone fields; and to improve data assimilation products through the provision of accurate, high resolution ozone profiles. Our early efforts appear very promising.

2.2.4 Evolution of the Pinatubo Cloud

The measurements of EOS AM's Measurements of Pollution in the Troposphere (MOPITT) instrument will produce low vertical resolution CO profiles and column CH₄ measurements. The Ozone Dynamic Ultraviolet Spectrometer (ODUS), scheduled for the EOS CHEM payload, will produce column ozone. We have developed a new method using trajectories which allows us to reconstruct the vertical structure of trace gases from column measurements under certain conditions. The column can be thought of as a shadow or projection of the three-dimensional field. The time evolution of the projection along with the column information can be used to reconstruct the three-dimensional field. We combine the various projections (like a medical CAT scan) to estimate the three-dimensional structure. The technique is an improvement of the method originally developed by Schoeberl et al. [1992c]. The new technique has been applied to the SO₂ field from the Pinatubo cloud as measured by TOMS with excellent results. We are currently preparing a paper on the technique.

2.2.5 Two Dimensional Modelling studies

2.2.5.1 Monte Carlo studies (new section)

As an outgrowth of studies started under the AEAP program and continued with ACMAP funding, we are now applying our Monte Carlo uncertainty study to 2D modeling of the evolution of ozone over the past two decades. As we try to understand the detailed mechanism responsible for the observed trend in ozone, it is important to consider the uncertainties inherent in the modeling as well as those in the measurements and the trend analysis. We have focussed thus far on the quantifiable part of model prediction uncertainty; that is the uncertainties due to input gas-phase chemical reaction rates, photolysis coefficients, heterogeneous reaction rates, and polar stratospheric cloud microphysics parameters. These have been propagated through a model calculation of the evolution of ozone over the past two decades. This model calculation included a realistic solar cycle and stratospheric sulfate aerosol variability. [Figure 2.2.5.1-1](#) shows the calculated time evolution of global total ozone from the nominal model using the accepted "best" values for input parameters compared to the TOMS version 7 data. Also shown are the 1-sigma uncertainty bounds using the estimated uncertainties in input parameters and the most extreme cases found.

The model calculated total ozone trend agrees quite well with the TOMS version 7 measurements. The differences between the model and measurements is less than the 1-sigma uncertainty of the model calculation. However, the model calculates a very small seasonal variation of the trend in the northern hemisphere midlatitudes in contrast to the data. This difference is many sigma from the mean calculated seasonal variation and cannot be attributed to input parameter uncertainties and there for most likely due to a deficiency of the model.

2.2.5.2 Interactive Two Dimensional Model Studies

Under this IDS, we have developed an interactive 2-D model based on the dynamics package of Bacmeister and Schoeberl [Bacmeister et al., 1995] to study long-term trends in trace gases. This model fully couples chemistry dynamics and radiation, and thus can be used to study the feedbacks between the processes which we have not been able to study with the fixed circulation 2-D model. Over the last year, several improvements have been made in the model. A new parameterization for chemistry occurring on the surfaces of polar stratospheric clouds has been added to the chemistry package, allowing the model to predict the Antarctic ozone hole. Extensive tuning of the planetary wave forcing parameters was carried out in order to improve the breakup of the southern hemisphere polar vortex. A gravity wave scheme has been added to the dynamics package (Bacmeister et al., 1995). The CO₂ infrared cooling parameterization of M.D. Chou and Kouvaris (1991) has been added to the radiation package, allowing the variation of the CO₂ heating rate calculation. The parameterization of Rosenfield (1992) for the radiative heating due to water ice and nitric acid trihydrate stratospheric clouds has been included. The chemistry package has been upgraded and is now compatible with that used by the 2-D assessment model.

The 2-D interactive model was used to study the effects of the sulfate aerosol cloud formed by the eruption of Mt. Pinatubo in June 1991 on stratospheric temperatures, dynamics, and chemistry (Rosenfield et al., 1996). Aerosol extinctions and surface area densities, constrained by satellite observations, were used to compute the aerosol effects on radiative heating rates, photolysis rates, and heterogeneous chemistry. The net predicted perturbations to the column ozone amount, shown in [Fig. 2.2.5.2-1](#), were low latitude depletions of 2-3% and northern and southern high latitude depletions of 10-12%, in good agreement with observations. In the low latitudes a depletion of roughly 1-2% was due to the altered circulation (increased upwelling) resulting from the perturbation of the heating rates, with the heterogeneous chemistry and photolysis rate perturbations contribution roughly 0.5% each. In the high latitudes the computed ozone column depletions were mainly a result of heterogeneous chemistry occurring on the surfaces of the volcanic aerosol. Computed global average ozone losses ([Fig. 2.2.5.2-2](#)) reached 1% at the end of 1991, and fell to a low of 3.2% around September 1992, after which the ozone began recovering. These computed global ozone changes were generally within 1% in absolute magnitude of those observed by the TOMS instrument except in early 1993 when the model ozone starts recovering faster than the observations indicate.

2.2.6 Mixing and Dynamics in the Stratosphere (New Section)

A significant effort has been devoted to an investigation of the vertical mixing of tracers which arises from the variability in the radiative heating of air parcels. Air parcels starting on a given isentropic surface experience different time histories of diabatic heating which causes irreversible vertical mixing across isentropic surfaces. We refer to this process as "diabatic dispersion".

We have investigated diabatic dispersion in the lower stratosphere by computing parcel trajectories initialized uniformly over the 500K surface on 1 Jan 1993. Parcels were followed for two months using analyzed winds and diabatic heating rates computed from analyzed temperatures. Two independent data sets and radiative calculations were used. The trajectory statistics suggest that the four regions, polar

vortex, winter hemisphere surf zone, tropics and extratropical summer hemisphere, are to some extent isolated from each other by eddy transport barriers. By looking at the mixing in each of these regions separately, we were able to establish the dependence of the vertical mixing on the horizontal transport and the spatial structure of the diabatic heating. We have found that the character and magnitude of the diabatic dispersion for parcels remaining in each of these four regions is distinctly different. The dispersion in both the surf zone and southern hemisphere extratropics is initially advective, but becomes diffusive after about one month with a diffusivity in the range 3-6 K²/day. Diabatic dispersion within the tropics and polar vortex over the two month period is more than an order of magnitude smaller and is less clearly diffusive. The potential temperature variance for the entire ensemble is dominated by differential advection associated with the mean diabatic circulation and increases quadratically with time. Our results therefore do not support the notion of global diffusive dispersion, at least not on seasonal time scales.

Other projects are underway which utilize the statistical information contained in observations of tracer and dynamical variability. The results of these investigations will be useful for a number of problems. As an example, we show here how a statistical comparison of tropical and midlatitude variability can be used to extract information about the strength of the transport barrier between the tropics and the northern midlatitudes. [Figure 2.2.6-1](#) shows the tropical and midlatitude mixing ratio PDFs (probability distribution functions) of N₂O observations taken by the CLAES instrument on UARS. The tropical and midlatitude PDFs shown here are histograms of N₂O observations in the latitude ranges 15S-15N and 15N-55N, respectively, at the altitudes 24,30 and 38 km, and during the period March 8-14, 1993. A scatter plot of mixing ratio versus latitude of the observations is shown below each PDF plot. The tropics and midlatitudes, as defined here, are also indicated on the plot.

The distributions are clearly more distinct at 30 km relative to the other two levels, indicating a stronger barrier to mixing across the latitude 15N. A measure of the barrier strength might be defined by quantifying the extent to which the tropical and midlatitude regions are chemically distinct, that is, the extent to which the two PDFs are resolved. A standard measure of the degree to which two overlapping distributions are distinct is the quantity "d" which is the absolute value of the difference in the mean values for each distribution, divided by the geometric mean of the variances of the distributions.

We have computed d as a function of altitude from CLAES N₂O observations for two different north facing periods Dec 8-15 1992, and March 8-14, 1993. The results are shown in [Figure 2.2.6-2](#) and indicate that the tropics and midlatitudes are most chemically distinct near 30km for the early March period. For the early December period on the other hand, d depends weakly on altitude in the range 25-35 km. In both cases, d decreases with increasing altitude. While this is partly due to the weakening of the transport barrier, it is also due to the greater photochemical loss of N₂O in the tropics. This causes the tropical PDF to move toward lower midlatitude values which also causes the regions to become less chemically distinct. All of these results are fairly insensitive to the choice of the northern tropical boundary, provided it is in the range 10N-20N.

The CLAES observations can be directly compared to model data by a similar analysis applied to model tracer fields interpolated to UARS measurement locations. Preliminary results indicate for example that the barrier strength in the GSFC chemistry and transport model during northern hemisphere winter is strongest at 25 km.

2.3 Stratospheric Data Assimilation

2.3.1 Chemical Assimilation

In the last EOS IDS report, the development of the Kalman filter for stratospheric constituent assimilation was reported. This work is now accepted for publication [Lyster et al. 1996]. The initial results for constituent assimilation were also presented at an international conference [Menard et al., 1995].

Since the last EOS IDS report we have performed extensive runs using real winds and data that have been retrieved from the UARS satellite. These runs are validations of the effectiveness of the Kalman filter approach. For example, a distinctive wave-breaking event is evident in stratospheric constituent observations in the period September 6-14 1992. [Figure 2.3.1-1](#) shows an attempt to reproduce this event using a pure forecast of methane from simple (zonally averaged) initial conditions. [Figure 2.3.1-2](#) shows an assimilation using the Kalman filter with a limited data set from the HALOE instrument (the black triangles show the locations of the observations). The wave-breaking is evident in the southern hemisphere, and it is absent from the first figure. A validation against CLAES data show that the structure of the event is being reproduced even where HALOE observations are not present.

Apart from the work using real data, there has been development in the methodology of the constituent Kalman filter. A key advantage of the Kalman filter is the ability to assess the accuracy of the assimilation (i.e., to calculate the error bars). We have implemented an approach for including the effects of errors in the assimilating wind. The winds are obtained from the DAO assimilation system (GEOS DAS) and the appropriate inclusion of their errors must be done in order to properly interpret the results of the constituent assimilation. Also, a common assumption in data assimilation is that errors are normally (Gaussian) distributed. This is inappropriate for constituent assimilation because the resulting field is (by definition) positive. We have developed a methodology for the log normal filter [Cohn, 1995] that removes this problem by transporting and assimilating the logarithm of the constituent field. We are also in the process of developing an extension to trajectory mapping called the Lagrangian filter. This approach to constituent assimilation takes into account the statistics of errors of the observations and the spatial correlation in the tracer field; in this approach observations now update the field in a group of neighboring parcels.

We have initiated a project to use the Kalman filter to map the three-dimensional structure of ozone in the lower stratosphere. This is a difficult project because of the spatial and temporal sparsity of data from satellites such as HALOE and SAGE. Also, the retrieval algorithms for these instruments have reduced accuracy in the vicinity of and below the ozone maximum in the lower stratosphere. We will use the Kalman filter to study the three dimensional development of structures such as the one shown in [Figure 2.3-2](#). Ultimately data such as these and total ozone measurements from TOMS instruments might be useful for mapping the distributions of tropospheric ozone. This approach will also be investigated.

2.3.2 Improvements to Assimilation System

A part of this IDS consists of diagnostic and transport studies designed to provide guidance to the DAO's data assimilation system development. These IDS studies make use of the available assimilation runs, completed for the UARS mission and aircraft missions, as well as special assimilation development runs. The diagnostic studies include the calculation of the residual mean circulation and comparisons of assimilation produced potential vorticity (pv) fields with tracer measurements from UARS. DAO winds and temperatures have been compared with UKMO winds and temperatures (Coy and Swinbank, submitted to JGR), with respect to diagnostic transport quantities, such as the representation of the polar pv barrier and the mean transport circulation. RDF trajectory model runs conserving pv and the 3D chemistry transport model for N₂O have been run for several DAO assimilations of a given time period, each experiment varying an aspect of the data assimilation system. Transport and trajectory studies based on changing the horizontal resolution of the analysis have shown that alternate methods of data insertion, such as BIAU (Balanced Incremental Analysis Update), can

reduce unphysical small scale structure in the assimilation produced winds without adversely affecting the transport results.

The stratospheric trajectory, transport, and diagnostic studies associated with this IDS, have played a large role in the development of the DAO's data assimilation system. One dramatic past improvement of the data assimilation system's GCM (General Circulation Model) has been the development and inclusion of the rotated computational pole. Moving the computational pole away from the geographic pole was done in direct response to stratospheric transport needs for clean cross polar transport during large amplitude stratospheric wave events. More recently, difficulties with 3D transport near the upper level of the transport model has been the major reason for the vertical expansion of the assimilation system's GCM from 60 to 80 km. In addition, the lack of polar vortex descent in the 3D transport model has required the inclusion of a simple orographic gravity wave model and a mesospheric Rayleigh friction drag term. The newest DAO assimilation system (GEOS-2) will contain all of the above GCM improvements. Moreover, trajectory, transport, and diagnostic studies done under this IDS have also highlighted problems with the assimilation's tropical wind analyses. These assimilation driven results generally show more small scale structure than is observed. Such results are believed to highlight a fundamental limitation of the current analysis system and have been a part of the rationale for using a completely new analysis system, PSAS (Physical space Statistical Analysis System), in the developing GEOS-2 assimilation system. Work under this IDS will continue, in collaboration with the DAO, to assess of the ability of assimilation winds to drive realistic transport and to provide supporting evidence from such studies to help guide future improvements to the data assimilation system.

2.4 Tropospheric Chemistry Studies

We have continued developing methods to derive tropical tropospheric ozone maps from TOMS and other satellites. As per last year's progress report, our first FY96 activity was to extend the method of Kim et al [1996] for deriving monthly averaged tropospheric ozone maps from TOMS between 10N and 10S to all of 1992 [Hudson and Thompson, 1996]. This latitude range is selected to correspond to tropical air masses only because studies with geopotential height show that sub-tropical air frequently penetrates equatorward of 15 degrees [Frolov and Hudson, 1996]. Accurate retrieval of time-averaged tropospheric ozone from TOMS requires stratospheric ozone to be relatively constant over time, which is the case in the tropics. Furthermore, because the stratospheric ozone retrieval is 100% efficient in the tropics, tropospheric ozone column amount can be derived without detailed knowledge of the stratospheric ozone profile [Hudson and Kim, 1994].

For tropospheric air masses, a good assumption is that the minimum tropospheric ozone column in the tropics is 26 DU [Komhyr et al, 1994; Thompson et al, 1996a], although some tropical ozonesondes launched over the Indian and central Pacific Oceans been as low as 10 DU [R. R. Dickerson, personal communication, 1995]. In addition, a striking feature of total ozone is a year- round wave-one pattern, with a maximum over the central Atlantic and a minimum over the central Pacific [Hudson and Thompson, 1996; Ziemke et al, 1996]. This can be verified with the tropical ozonesonde record, although the latter is very incomplete. For the years, 1991-1992, for which sonde coverage at Natal (5.5S, 35W), Ascension (8S, 14W), and Brazzaville (4S, 15E) captures total ozone over the Atlantic [Thompson et al, 1996a,b], there are no Pacific sondes. For 1986-1990 there is a record at American Samoa (14S, 174W) [Komhyr et al, 1994], but this site is not always in the tropical band.

The wave-like pattern is used to derive a tropospheric ozone field by two methods [Kim et al, 1996], with an efficiency correction for low-lying ozone at high concentrations, as observed during biomass burning [Thompson et al, 1996b]. In one method, it is assumed (1) that the background total ozone column over the Pacific, consists of Strat. O3 Col. + 26 DU, and is zonally constant, and (2) that any

excess ozone beyond that amount is in the troposphere. This implies, however, that tropospheric column ozone is > 65 DU over Africa during the August-October biomass burning period (Fig. 2.4-1), with an Indian Ocean background of 45 DU. These levels are 15-20 DU higher than suggested by in-situ measurements during TRACE-A [Baldy et al, 1996; Fishman et al, 1996; Browell et al, 1996; Thompson et al, 1996b].

The alternative technique assumes that the total "background ozone" consists of a stratospheric wave, plus a zonally constant 26 DU. During biomass burning season, an additional "hump" is superimposed on the background wave over the Atlantic and tropospheric column ozone over the burning regions of Africa and South America is 45-50 DU during 1992, for example, in agreement with the sonde record (Fig. 2.4-1; Kimet al, 1996). The picture obtained assuming a stratospheric wave in March-April-May also agrees very well with the Ascension, Brazzaville and Natal sondes in 1992, whereas the tropospheric wave assumption does not (Fig. 2.4-2). These results appear to contradict the inferences from the sondes, as described by Ziemke et al [1996], and we are seeking independent approaches to determining the nature of the wave-like pattern. These include further analysis with sample tropospheric ozone profiles - what radiances and total ozone are derived, given various assumptions of stratospheric ozone? In addition, we will start to look at ozone in the tropical lower stratosphere-upper troposphere from the 3D chemical model for insight into dynamical contributions to the wave pattern.

One thing is certain from the analyses to date. Validation of alternative approaches for deriving tropospheric ozone requires a good ozonesonde network in the tropics. The record coincident with Nimbus 7 TOMS is too spotty. During its 14-plus-year record, Natal was the only continuously operational sounding station within 10 degrees of the equator. Also needed are a central Atlantic and/or Africa site (Ascension is ideal; Brazzaville would also work, although it suffers from more variable cloud effects; Thompson et al, 1996b). In the Pacific, locations that have been suggested are Galapagos, Christmas Island (F. Hasebe personal communication, 1996) and Tarawa (W. A. Matthews, personal communication, 1996). Now that ADEOS- and EarthProbe-TOMS are operational, we can continue development of tropical tropospheric ozone retrievals on a firmer basis if the sonde network is enhanced.

The second FY96 activity is the production of the entire 14-year Nimbus 7 TOMS tropical tropospheric ozone map record to see if there are trends discernable during this time. Total ozone maps, prepared as in Kim et al [1996], have just been completed.

As part of this IDS, complementary activities to the production of tropospheric ozone maps are analyses of in-situ tropospheric ozone and related data and modeling and analysis of the convection-ozone link. Three recently completed papers on transport and chemistry associated with southern African ozone (south of 20S) [Swap et al, 1996; Thompson et al, 1996c; Tyson et al, 1996] further elucidated the photochemical origins of persistent ozone layers over the subtropics during the SAFARI/TRACE-A period (September-October 1992). African biomass burning is not the only source. Near-surface tracer measurements at Etosha Park signified industrial and/or biogenic sources as well [Swap et al, 1996]. In the upper troposphere (10-15 km) ozonesondes at Pretoria (25S, 28E) and Etosha Park (19S, 16E) averaged 3-4 DU richer in September-October 1992 than in March-April-May and back trajectories for every one of the 30 sondes taken during SAFARI/TRACE-A showed origins 4-8 days earlier over South America. The mechanism for this ozone source is presumably post-convective ozone formation from pyrogenic, biogenic and/or urban NO_x and CO sources.

We are looking at ozone and biomass fire links in SCAR-B [Smoke, Clouds, Aerosols, and Radiation-Brazil, M. King and Y. Kaufman, NASAPIs], a MODIS-sponsored biomass burning experiment conducted in August-September 1995 [Thompson et al, 1996d]. Unfortunately, SCAR-B occurred during the gap between Nimbus/Meteor TOMS coverage and EP/ADEOS TOMS so it does not help in further TOMS tropospheric ozone map development. As part of this IDS, improvements to the GEOS-1

tracer model convective parameterization were performed [Allen et al., 1996] and a review paper on the tropical ozone-convection link was completed [Thompson et al., 1996e].

2.5 Other Activities

The section below summarizes some of the other activities supported by this IDS. These research efforts do not fall under the categories described above but are an important part of this investigation.

2.5.1 TOTE/VOTE Analysis (New Section)

During the December 1995/ January-February 1996, the PI was also the Project Scientist for the Tropical Ozone Transport Experiment/Vortex Ozone Transport Experiment (TOTE/VOTE). We are now beginning to analyze the data from that mission..One of the most interesting observations made was the presence of sub-visible cirrus south of 18N at the longitude of Hawaii. [Figure 2.5.1-1](#) shows an example of the DIAL aerosol observations made on the flight. Jensen et al [1996] have speculated that subvisible cirrus near the tropopause might generate broad scale uplift and hence allow air to enter the stratosphere. This hypothesis is a variant on Danielsen's idea that the heating of the cirrus shields in tropical systems can radiatively lift air to stratospheric potential temperatures. The exciting discovery here is that the cirrus observed is not attached to any nearby convective systems.

We are also analyzing other aspects of the TOTE/VOTE data including polar ozone depletion, mixing in the stratosphere, and aircraft exhaust studies.

2.5.2 HIRDLS simulation studies

The HIRDLS instrument on the EOS CHEM platform is designed to make horizontal and vertical observations at higher resolutions than have previously been made, while observing the upper troposphere and lower stratosphere with improved sensitivity and accuracy. The higher horizontal resolution is achieved by azimuthal scanning of the instrument's field of view. Previous limb-viewing sounders (LIMS, ISAMS, CLAES, MILS, etc.) did not have this azimuthal scanning capability and thus were unable to sample a given latitude circle more than twice per orbit.

High-resolution (1 degree by 1 degree) global RDF fields have now been generated on the 560 K isentropic surface, covering every six hours for 30 days, from February 19, 1992, to March 19, 1992. The fields are currently being used to examine scale-dependent statistics. These fields will be used for simulations of satellite sampling strategies, permitting more realistic investigations of how satellite instruments sample an evolving high-resolution meteorological field. The results of this work culminated in a M.S. Thesis.

2.5.3 TOMS data

Aside from UARS data, investigators under this IDS spend some time looking at TOMS data and performing analysis of global ozone amounts. Simulations of ozone change have to fit within the TOMS observational set. A TOMS-like instrument (ODUS) will be launched on EOS CHEM. We are currently analyzing new data from ADEOS and Earth Probe TOMS, [Figure 2.5.3-1](#) shows differences between the data sets. Most of the differences can be accounted for by changes in small scale meteorological processes that occur between satellite crossing times. However there are larger scale differences that are still under investigation.

2.5.4 Analysis of CRISTA data

CRISTA is an IR limb stratosphere chemistry sounder which flew on the shuttle ATLAS missions. We have been working with Dr. Offermann of Wuppertal University to help analyze the data. Preliminary calculations show good agreement between the high horizontal resolution CRISTA data and RDF simulations of tracer fields. Unfortunately the first CRISTA data set has not been released (release was targeted for June 1996) so the analysis has not been completed.

FIGURE CAPTIONS

[Fig. 2.1.1-1](#) Summary of model results from MODE [Schoeberl et al., 1996] showing the change in total ozone as a function of year for the Antarctic ozone hole.

[Fig. 2.1.2-1a](#) and [Fig. 2.1.2-1b](#) Summary of preliminary Arctic model results from MODE showing the change in ozone and other trace gases compared with observations from Jan. to Feb. 1993. Part a, ozone comparisons; part b, ClONO₂, HNO₃, HCl and PV.

[Fig. 2.2.1-1](#) Observations of ozone from HALOE (month of February), CLAES (Feb. 19) and MILS (Feb. 19) compared with model mixing ratios interpolated to the time and location of the satellite measurements.

[Fig. 2.2.1-2](#) The model ozone at 6.8 hPa illustrating horizontal variability. This variability is reflected in the model/observation comparisons shown in Figure 2.2.1-1.

[Fig. 2.2.2.1-1](#) The ratio of CLAES N₂O/CH₄ averaged between 8N and 8S (in color) with time mean removed (at right). Dark lines show the Singapore zonal winds. Phase lags/leads of one and two months are shown in white.

[Fig. 2.2.3-1](#) Typical midlatitude SAGE ozone profile showing number density as a function of altitude. Most of the ozone falls between the 400K (20km) and 1200K (36km) potential temperature levels (marked in the figure).

[Fig. 2.2.3-2](#) Total column ozone as derived from combined stratospheric measurements made by SAGE and HALOE. The trajectory mapping technique has been applied to data from both instruments to produce this synoptic map of the ozone distribution in September 1994.

[Fig. 2.2.3-3](#) Comparison of HALOE and SAGE ozone measurements at 600K (26km) using the trajectory mapping technique.

[Fig. 2.2.3-4](#). TOMS total ozone field for the same date shown using the HALOE/SAGE data in Figure 2.

[Fig. 2.2.5.1-1](#) The calculated time evolution of global total ozone from the nominal 2D model using the accepted "best" values for input parameters compared to the TOMS version 7 data (solid line), 1-sigma uncertainty bounds using the estimated uncertainties (dashed line) in input parameters, and the most extreme cases found (dotted lines).

[Fig. 2.2.5.2-1](#) Percent changes in column ozone due to full chemistry and radiation perturbation. Contour intervals are -28, -24, -20, -16, -12, -8, -4, -3, -2, 0, 2, 4.

[Fig. 2.2.5.2-2](#) Global average ozone percent changes with full perturbation compared to TOMS.

[Figure 2.2.6-1](#) Tropical and midlatitude CLAES v.7 N20 PDFs (probability distribution functions) and latitude/mixing ratio scatter plots at vertical levels 24, 30 and 38 km, for March 8-15, 1993. The vertical lines in the scatter plots indicate the boundaries of the tropics and midlatitudes as defined here.

[Figure 2.2.6-2](#) The altitude dependence of the difference between the tropical and northern midlatitude N20 tracer distributions. CLAES vs N20, March 8-15, 1993.

[Fig. 2.3.1-1](#) A constituent forecast of methane from simple (zonally averaged) initial conditions.

[Fig. 2.3.1-2](#) An assimilation of CH₄ using the Kalman filter with a limited data set from the HALOE instrument (the black triangles show the locations of the observations).

[Fig. 2.4-1](#) Two maps of tropospheric ozone column for October 1992 in Dobson units (DU) [Hudson and Thompson, 1996]. Methods of deriving the maps are described in Kim et al [1996]. The upper frame is based on assuming the wavelike pattern in total ozone is due to a tropospheric wave. The lower frame assumes that the Two maps of tropospheric ozone column for May 1992 in Dobson units (DU) [Hudson and Thompson, 1996].

[Fig. 2.4-2](#) Two maps of tropospheric ozone column for May 1992 in Dobson units (DU) [Hudson and Thompson, 1996]. Methods of deriving the maps are described in Kim et al [1996]. The upper frame is based on assuming the wavelike pattern in total ozone is due to a tropospheric wave. The lower frame assumes that the wavelike pattern is in the stratosphere. Ozonesonde data in March-April-May for 1992 shows average tropospheric ozone column at Ascension Island (8S, 14W) was 30 DU and at Brazzaville (4S, 15E), the sondes averaged 34 DU. These values agree better

[Fig. 2.5.1-1](#) DIAL observations of aerosols for the TOTE flight of Dec. 15, 1995. Overlaid are the MTP temperatures. The high scattering features show sub-visible cirrus near the tropopause.

[Fig. 2.5.3-1](#) Column ozone differences between Earth Probe and ADEOS TOMS on Oct. 1, 1996. Because of the lower orbit altitude, Earth Probe TOMS cannot scan from orbit track to orbit track.

References

- Allen, D. J., P. Kasibhatla, A. M. Thompson, R. B. Rood, B. Doddridge, K. E. Pickering, R. D. Hudson and S-J. Lin, *J. Geophys. Res.*, Transport-induced interannual variability of carbon monoxide determined with a chemistry and transport model, *J. Geophys. Res.*, submitted, 1996.
- Bacmeister, J.T., M.R. Schoeberl, M.E. Summers, J.E. Rosenfield, and X. Zhu, Descent of long-lived trace gases in the winter polar vortex, *J. Geophys. Res.*, *100*, 11,669-11,684, 1
- Bacmeister, J. T., S. D. Eckermann, L. Sparling, K. R. Chan, M. Loewenstein, and M. H. Proffitt, 1996: Analysis of intermittency in aircraft measurements of velocity, temperature and atmospheric tracers using wavelet transforms, To appear in *NATO ASI Series, Vol. 1, Gravity Wave Processes and their Parameterization in Global Climate Models*, ed. K. P. Hamilton, Springer Verlag, Heidelberg.
- Browell, E. V., et al, Air mass characteristics observed over the tropical Atlantic, Africa, and Brazil during TRACE-A, *J. Geophys. Res.*, in press, 1996.
- Chou, M.-D., and L. Kouvaris, Calculations of transmission functions in the infrared CO₂ and O₃ bands, *J. Geophys. Res.*, *96*, 9003-9012, 1991. 995.

- Cohn, S.E., 1996: An introduction to estimation theory. Special issue dedicated to data assimilation in meteorology and oceanography: theory and practice, submitted to *J. Met. Soc. Japan*.
- Considine, D.B., R.S. Stolarski, C.H. Jackman, J.E. Rosenfield, and E.L. Fleming, "Uncertainty in the response of ozone to chlorine increases in a 2D model of stratospheric photochemistry", submitted to the proceedings of the Quadrennial Ozone Symposium, L'Aquila, Italy, September, 1996.
- Coy, L., and R. Swinbank, The characteristics of stratospheric winds and temperatures produced by data assimilation, submitted to *JGR*.
- Douglass, A. R., R. B. Rood, S. R. Kawa, D. J. Allen, M. C. Cerniglia, Simulation of the evolution of the middle latitude winter ozone in the middle stratosphere, submitted (almost) to *J. Geophys. Res.*, 1996.
- Fishman, J., V. G. Brackett, E. V. Browell, and W. B. Grant, Tropospheric ozone derived from TOMS/SBUV measurements during TRACE-A, *J. Geophys. Res.*, in press, 1996.
- Frolov, A. D., and R. D. Hudson, Correlation of northern hemisphere total ozone and geopotential height fields, in *XVIII Quadrennial Ozone Symposium Abstract Volume*, L'Aquila, Italy, 12-21 Sept. 1996, p. 173.
- Hudson, R. D., and J. Kim, Direct measurements of tropospheric O₃ using TOMS data, in *Ozone in the Troposphere and Stratosphere*, ed. R. D. Hudson, *NASA Conf. Pub. 3266*, pp.119-121, 1994.
- Hudson R. D., J-H. Kim, and A. M. Thompson, On the derivation of tropospheric column ozone from radiances measured by the Total Ozone Mapping Spectrometer, *J. Geophys. Res.*, *100*, 11137-11146, 1995.
- Hudson, R. D., and A. M. Thompson, Annual cycle of tropospheric ozone in the tropics, in *XVIII Quadrennial Ozone Symposium Abstract Volume*, L'Aquila, Italy, 12-21 Sept. 1996, p. 240.
- Jensen, E. J., O. B. Toon, J. D. Spinhirne and H. B. Selkirk, On the formation and persistence of subvisible cirrus clouds near the tropical tropopause, *J. Geophys. Res.*, in press, 1996.
- Kim J. H., R. D. Hudson, and A. M. Thompson, Derivation of time-averaged tropospheric column ozone from radiances measured by the Total Ozone Mapping Spectrometer: Intercomparison and analysis, *J. Geophys. Res.*, *101*, in press, 1996.
- Komhyr, W. D., S. J. Oltmans, J. A. Lathrop, J. B. Kerr, and W.A. Mathews, The latitudinal distribution of ozone to 35 km altitude from ECC ozonesonde observations: 1982-1990, in *Ozone in the Troposphere and Stratosphere*, ed. by R. D. Hudson, *NASA Conf. Pub. 3266*, pp. 858-862, 1994.
- Lyster, P.M. , S.E. Cohn, R. Menard, L.-P. Chang, S.-J. Lin, R. Olsen, 1996: Parallel Implementation of a Kalman Filter for Constituent Data Assimilation, accepted for publication in *Mon. Wea. Rev.*, 1996.
- Manney, G. L., L. Froidevaux, J. W. Waters, R. W. Zurek, J. C. Gille, J. B. Kumer, J. L. Mergenthaler, A. E. Roche, A. O'Neill, R. Swinbank, Formation of low-ozone pockets in the middle stratospheric anticyclone during winter, *J. Geophys. Res.*, *100*, 13,939-13,950, 1995
- Menard, R., P.M. Lyster, L.-P. Chang, and S.E. Cohn, 1995: Middle atmosphere assimilation of UARS

constituent data using Kalman filtering: preliminary results. Second International Symposium on Assimilation of Observations in *Meteorology and Oceanography, Tokyo, 13-17 March 1995, World Meteorological Organization*, pp 235-238.

Morris, G.A., et al., Trajectory mapping and applications to data from the Upper Atmosphere Research Satellite, *J. Geophys. Res.*, 100,16,491--16,505, 1995.

Rosenfield, J.E., Radiative effects of polar stratospheric clouds during the Airborne Antarctic Ozone Experiment and the Airborne Arctic Stratospheric Expedition, *J. Geophys. Res.*, 7841-7858, 1992.

Schoeberl, M. R. et al., An estimate of the dynamical isolation of the tropical lower stratosphere using UARS wind and trace gas observations of the Quasi-biennial Oscillation, *Geophys. Res. Lett.*, (in press), 1996.

Schoeberl, M. R. et al., Development of the Antarctic ozone hole, *J. Geophys. Res.*, 101, 20909-20924, 1996.

Swap, R. J., A. M. Thompson, M. Garstang, and S. A. Macko, Multiple sources of southern African ozone in the lower troposphere during biomass burning, *Geophys. Res. Lett.*, submitted, 1996.

Thompson, A. M., R. D. Diab, G. E. Bodeker, M. Zunckel, G. J. R. Coetzee, C. B. Archer, D. P. McNamara, K. E. Pickering, J. B. Combrink, J. Fishman, and D. Nganga, Ozone over southern Africa during SAFARI/TRACE-A, *J. Geophys. Res.*, in press, 1996a.

Thompson, A. M., K. E. Pickering, D. P. McNamara, M. R. Schoeberl, R. D. Hudson, J. H. Kim, E. V. Browell, V. W. J. H. Kirchhoff, and D. Nganga, Where did tropospheric ozone over southern Africa and the tropical Atlantic come from in October 1992? Insights from TOMS, GTE/TRACE-A and SAFARI-92, *J. Geophys. Res.*, in press, 1996b.

Thompson, A. M., D. P. McNamara, R. J. Swap, J. Combrink, and R. D. Diab, Sources of free tropospheric ozone in subtropical southern Africa during SAFARI-92/TRACE-A: Intra- and inter-continental transport, *J. Geophys. Res.*, submitted, 1996c.

Thompson, A. M., D. P. McNamara, V. W. J. H. Kirchhoff, and A. Setzer, Tropospheric ozone at Cuiabá during SCAR-B and TRACE-A, in *Proceedings of SCAR-B AEB Workshop*, Fortaleza, Brazil, Nov. 1996d.

Thompson, A. M., W.-K. Tao, K. E. Pickering, J. R. Scala, and J. Simpson, Tropical deep convection and ozone formation, *Bull. Am. Meteor. Soc.*, submitted, 1996e.

Tyson, P. D., M. Garstang, A. M. Thompson, P. C. D'Abreton, R. D. Diab and E. V. Browell, Transport and photochemistry of ozone over south central southern Africa during SAFARI, *J. Geophys. Res.*, submitted, 1996.

Ziemke, J. R., S. Chandra, A. M. Thompson, and D. P. McNamara, Zonal asymmetries in southern hemisphere column ozone: Implications of biomass burning, *J. Geophys. Res.*, 101, 14421-14427, 1996.

New Publications under this IDS

- (1) Calculations of the Stratospheric QBO for Time-Varying Wave Forcing, by M. A. Geller, W. Shen, M. Zhang, and W. Wu, To appear in *J. Atmos. Sci.*, 1996.
- (2) Stratospheric Acceleration from Tropical Waves Driven by Moist Convection and Extratropical Wave Forcings, by W. Shen and M. A. Geller, submitted to *J. Atmos. Sci.*, 1996.
- (3) Lyster, P.M. , S.E. Cohn, R. Menard, L.-P. Chang, S.-J. Lin, R. Olsen, 1996: Parallel Implementation of a Kalman Filter for Constituent Data Assimilation, accepted for publication in *Mon. Wea. Rev.*, 1996.
- (4) Schoeberl, M. R. et al., An estimate of the dynamical isolation of the tropical lower stratosphere using UARS wind and trace gas observations of the Quasi-biennial Oscillation, *Geophys. Res. Lett.*, (in press), 1996.
- (5) Schoeberl, M. R. et al., Development of the Antarctic ozone hole, *J. Geophys. Res.*, *101*, 20909-20924, 1996.
- (6) Sparling, L. C., J. A. Kettleborough, P. H. Haynes, M. E. McIntyre, J. E. Rosenfield, P. A. Newman and M. R. Schoeberl, Diabatic dispersion in the lower stratosphere, *Journal of Atmospheric Sciences*, submitted, 1966
- (7) Allen, D. J., P. Kasibhatla, A. M. Thompson, R. B. Rood, B. Doddridge, K. E. Pickering, R. D. Hudson and S.-J. Lin, *J. Geophys. Res.*, Transport-induced interannual variability of carbon monoxide determined with a chemistry and transport model, *J. Geophys. Res.*, submitted, 1996.
- (8) Thompson, A. M., W.-K. Tao, K. E. Pickering, J. R. Scala, and J. Simpson, Tropical deep convection and ozone formation, *Bull. Am. Meteor. Soc.*, submitted, 1996e.
- (9) Thompson, A. M., D. P. McNamara, R. J. Swap, J. Combrink, and R. D. Diab, Sources of free tropospheric ozone in subtropical southern Africa during SAFARI-92/TRACE-A: Intra- and inter-continental transport, *J. Geophys. Res.*, submitted, 1996c.
- (10) Lyster, P.M. , S.E. Cohn, R. Menard, L.-P. Chang, S.-J. Lin, R. Olsen, 1996: Parallel Implementation of a Kalman Filter for Constituent Data Assimilation, accepted for publication in *Mon. Wea. Rev.*, 1996.
- (11) Bacmeister, J. T., S. D. Eckermann, L. Sparling, K. R. Chan, M. Loewenstein, and M. H. Proffitt, 1996: Analysis of intermittency in aircraft measurements of velocity, temperature and atmospheric tracers using wavelet transforms, To appear in *NATO ASI Series, Vol. 1, Gravity Wave Processes and their Parameterization in Global Climate Models*, ed. K. P. Hamilton, Springer Verlag, Heidelberg.
- (12) Jackman, C.H., E.L. Fleming, S. Chandra, D.B. Considine, and J.E. Rosenfield, Past, present, and future modelled ozone trends with comparisons to observed trends, *J. Geophys. Res.*, 1996, in press.
- (13) Nash, E.R., P.A. Newman, J.E. Rosenfield, and M.R. Schoeberl, An objective determination of the polar vortex using Ertel's potential vorticity, *J. Geophys. Res.*, *101*, 9471-9478, 1996.
- (14) Newman, P.A. and J.E. Rosenfield, Stratospheric thermal damping times, *Geophys. Res. Lett.*, 1996, submitted.
- (15) Rosenfield, J.E., D.B. Considine, P.E. Meade, J.T. Bacmeister, C.H. Jackman, and M.R. Schoeberl,

Stratospheric effects of the Mt. Pinatubo aerosol studied with a coupled two-dimensional model, *J. Geophys. Res.*, 1996, submitted. or Constituent Data Assimilation, accepted for publication in *Mon. Wea. Rev.*, 1996.

(16) Newman et al. Measurements of polar vortex air in the midlatitudes, *J. Geophys. Res.*, 101, 12879-12891, 1996.

(17) Tabazadeh, A., O. B. Toon, B. L. Gary, J. T. Bacmeister, and M. R. Schoeberl, Observational constraints on the formation of Type 1a polar stratospheric clouds, *Geophys. Res. Lett.*, 23, 2109-2112, 1996.

(18) Coy, L., and R. Swinbank, The characteristics of stratospheric winds and temperatures produced by data assimilation, submitted to *JGR*, 1996.

Appendix: GSFC Automailer Statistics

The GSFC Automailer provides trajectory services to the scientific community. It is partially supported under this IDS. The collection of the meteorological data for this effort is funded under the Newman Data Support proposal. Computer costs and trajectory code maintenance is supported under this proposal. We also support a copy of the trajectory model code being run at NASA Ames to support other aircraft missions. Below is the most recent usage report.

GSFC /science Automailer Usage Report
Covering 1995-01-01 to 1995-12-31

USER	ACCESSES	USER	ACCESS
gobbi@sunifal	1	eharnett@u.washington.edu	2
vfioletov@dow.on.doe.ca	14	xliu@du.edu	2
matthias.lugauer@psi.ch	3	carole.deniel@aerov.jussieu.fr	13
pierluigi.calanca@empa.ch	5	deniel@aerov.jussieu.fr	5
ingold@sun.iap.unibe.ch	535	lezeaux@observ.u-bordeaux.fr	1
cadyp@aer.com	10	gilles@aloha.observ.u-bordeaux.fr	1
danilin@aer.com	178	ricaud@observ.u-bordeaux.fr	4
hsu@hoss.stx.com	1	hervig@mcmsun5.mcmurdo.gov	6
grooss@mpch-mainz.mpg.d400.de	9	s107@mcmsun5.mcmurdo.gov	23
trapp@mpch-mainz.mpg.d400.de	2	s131@mcmsun5.mcmurdo.gov	61
peter@diane.mpch-mainz.mpg.de	4	screwell@mcmsun5.mcmurdo.gov	153
bms@schalk.physik.uni-bremen.de	171	voemelho@mcmsun5.mcmurdo.gov	36
gerd@atm.physik.uni-bremen.de	1	ejensen@fog.arc.nasa.gov	10
jens@schalk.physik.uni-bremen.de	52	haddix@sundog.arc.nasa.gov	6
jo@schalk.physik.uni-bremen.de	67	hamill@light.arc.nasa.gov	70
tobias@atm.physik.uni-bremen.de	1	pfister@margie.arc.nasa.gov	1
zhang@asrc.albany.edu	43	taba@sky.arc.nasa.gov	90
atmosphys@uwyo.edu	169	grainger@local:.oxatm.dnet.nasa.gov	3
awhitten@uwyo.edu	10	lare@eos913c.gsfc.nasa.gov	16
lj@mercuri.gps.caltech.edu	11	huahu@alpha1.jpl.nasa.gov	1
randall%snooze@vaxf.colorado.edu	3	lyatt@alpha1.jpl.nasa.gov	189
djschnei@mtu.edu	198	bjohnson@cmdl.noaa.gov	11
dr. pierre fogal@phys.du.edu	1	donnelly@al.noaa.gov	2
blathe@owl.phys.du.edu	4	s107.mcmurdo@mcmurdo.gov	91
pfogal@grizzly.phys.du.edu	82	s107a.mcmurdo@mcmurdo.gov	6
dan@bottesini.harvard.edu	187	didonfra@hp.ifsia.fra.cnr.it	262
eric@bottesini.harvard.edu	43	ifsia.fra.cnr.it@ifsia.fra.cnr.it	2

weinstock@bottesini.harvard.edu	5	stefania@ifsi.fra.cnr.it	1
hlshocke@mtu.edu	10	pellegrini_a@casaccia.enea.it	53
jmshanno@mtu.edu	30	aellig@quate.nrl.navy.mil	26
kmurcray@du.edu	30	fromm@poam_a.nrl.navy.mil	61
usinski@essc.psu.edu	62	hornstei@poamb.nrl.navy.mil	4
dcheng@uars.sunysb.edu	302	mike@wvms.nrl.navy.mil	292
dshindell@uars.sunysb.edu	4	pauls@atlas.nrl.navy.mil	8
screwell@uars.sunysb.edu	338	siskind@ismap3.nrl.navy.mil	10
uklein@uars.sunysb.edu	229	toma@poamb.nrl.navy.mil	104
vyudin@uars.sunysb.edu	7	qlk@sron.rug.nl	1
jamesw@sanjuan.acd.ucar.edu	131	kreher@kea.lauder.cri.nz	19
blathe@meeker.ucar.edu	79	liley@kea.lauder.cri.nz	7
jamesw@acd.ucar.edu	65	kreher@lauder.niwa.cri.nz	16
katja@ash.mmm.ucar.edu	10	liley@lauder.niwa.cri.nz	60
renate@meeker.ucar.edu	103	attwell@atm.ox.ac.uk	36
hauer@marten.uwyo.edu	19	grainger@atm.ox.ac.uk	23
hervig@trex.uwyo.edu	46	lambert@atm.ox.ac.uk	2
johnson@grizzly.uwyo.edu	2	remedios@atm.ox.ac.uk	8
zhao@moose.uwyo.edu	3	coetzee@cirrus.sawb.gov.za	58

TOTALS: 92 users, 5136 accesses

FUNCTION	ACCESSES
curtain	428
metmaps	285
metprofile	1403
metxsects	59
plot_met	947
trajectory	2014
TOTAL:	5136

This averages to 14 jobs successfully run per day.

These figures represent a 53% increase in the number of users in 1995 over those for 1994, and a 29% increase in the number of jobs run.